

Designing A Pattern Stabilization Method Using Scleral Blood Vessels For Laser Eye Surgery

Aydın Kaya¹, Ahmet Burak Can¹, Hasan Basri Çakmak²

Hacettepe University, Department of Computer Engineering, Ankara, Turkey¹

Ataturk Research Hospital, Department of Ophthalmology, Ankara, Turkey²

{aydinkaya,abc}@cs.hacettepe.edu.tr, hbcakmak@gmail.com

Abstract— In laser eye surgery, the accuracy of operation depends on coherent eye tracking and registration techniques. Main approach used in image processing based eye trackers is extraction and tracking of pupil and limbus regions. In eye registration step, iris region features extracted from infrared images are used generally. Registration step determines the angular shift of eye origin by comparing the eye position on operation table with the eye topology obtained before the operation. Registration is only applied at the beginning but patient's movements don not stop during operation. Hence we presented a method for pattern stabilization which can be repeated during operation at regular intervals. We use scleral blood vessels as features due to texturedness and resistance to errors caused by pupil center shift and ablation of cornea region.

Keywords-component; feature extraction, scleral blood vessels, ocular biometrics.

I. INTRODUCTION

Loss of vision is one of the most disturbing physical illnesses that affect human life. Corneal disorders are frequently seen eye diseases; deformation on cornea causes focus-based vision degradation. External lenses are often used for solution but developing technology provides correction on corneal layer of eye with surgical intervention. The most applied surgical method is laser eye surgery (*refractive surgery*) which relies on reshaping corneal layer with densified laser light [1]. Although most patients barely move their eyes during operation, laser's lock up and maintaining visual axis position and the pattern to be applied on cornea have crucial importance in refractive surgery [2].

Image processing methods applied in this area can be divided in two categories: eye tracking during operation and eye registration on pre-operation. Firstly, cornea's detailed topography is extracted before the surgery. Eye registration or hand-marking ensure alignment of visual axis and pattern center, and compliance to the topography. This step is necessary to determine angular and translational changes of patient's eye on operation table. The most common eye

registration method used instead of hand-marking is iris registration [6] which uses iris region features to register images taken prior to operation and on the operation table. Eye tracking systems mostly use pupil or limbus position for tracking. There are laser-based, image-processing based or photoelectric-based eye tracking methods [4]. Even though eye tracking and iris-registration help maintaining the consistency of ablation, they have some handicaps. Some of the features that enable tracking and registration may disappear due to ablation and pupil center may shift [5] due to flexible structure of iris.

We proposed a method which can be used for pattern stabilization in laser eye surgery. This method is aimed to work at regular intervals to extend accuracy of registration process for entire operation. Scleral blood vessels are used as features to align control pattern's positional change. Thus, pattern stabilization can be more resistant to problems caused by changes in pupil and iris region during the operation. In our experiments, we observed this method can detect the eye movements with small error rates.

II. RELATED WORK

Eye tracking systems use primitive image processing methods to keep up with high speed laser. These systems usually illuminate eye with infrared light (IR), gather reflected light with IR-sensitive cameras and evaluate pupil's appearance for optic axis determination [2]. Various systems use the limbus (*iris margin*) and pupil's position for tracking [3]. Although these methods are adequate for speed requirements, two dimensional tracking cannot compensate human eye's movements and may cause lost of pattern center due to movements of patient and pupil [2]. These methods should be made more robust and independent from the condition of surgery environment.

The other problem that can't be solved by eye tracking is cyclotorsional movements of eye [7]. Cyclotorsion is defined as the rotation of eye around the anteroposterior axis [8]. Basically, human eye moves around z axis as well as x and y

axis direction. These movements occur especially when the patient’s head moves. Additionally, the difference of patient’s position between wavefront device and operation table causes torsional change. Primitive eye tracking methods cannot handle these changes. Chernyak’s innovative work iris registration [6] uses natural features on iris region and finds cyclotorsion angle. This method first enhances iris region with image processing methods, extracts salient features and then calculates angle by iris-unwrapping method. Iris registration is the only registration method available on laser systems and widely used in commercial products.

III. OUR APPROACH

In our method we applied well-known object tracking/recognition approach proposed by Lowe [10]. We identified the pattern as an object to track and assigned sclera blood vessel features as its descriptors. Our method includes the steps given in Figure 1. Firstly, reference image is obtained from the input video and a preprocessing step is applied to find the region of scleral blood vessels on this image. The features extracted by SIFT [9] algorithm are stored for matching the reference image with the subsequent images in the video. After processing the reference image, the following steps are gathering the subsequent image, extracting its features (without region of interest selection), matching it with the reference image, and model fitting after making the necessary calculations.

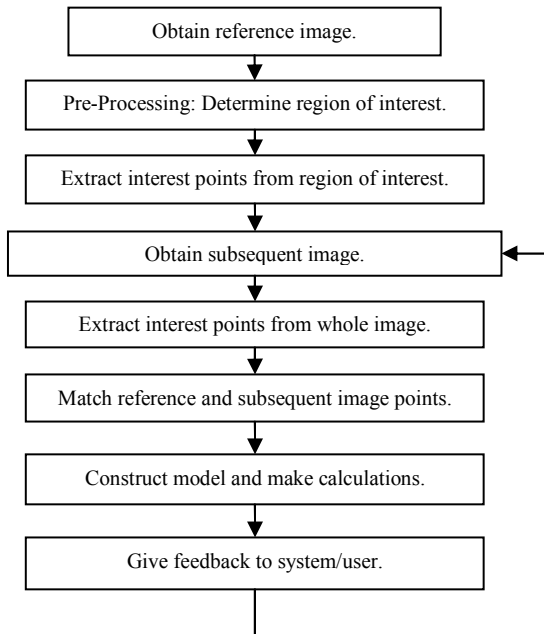


Figure 1: Flowchart of proposed method.

A. Data Sets

Data sets are acquired from Ataturk Research Hospital’s Ophthalmology department. Videos are captured by Scwind Eiris excimer laser’s camera, SONY XC-555P CCD, which is used for recording surgeries. Image resolution is 704x576 pixels in RGB format. For testing our approach, we created various data sets with images obtained at one second, ten seconds and sixty seconds intervals from videos.

B. Preprocessing

Region of scleral blood vessels must be salient since the features are extracted from this region. We examined grey level, green, red, blue channel images (Figure 2) for extraction of the required information –interest points. We eliminated the red and blue channel images due to low distinctiveness of vessels in the red channel and high brightness in the blue channel. Grey level and green channel images look similar according to feature detail but we got better matching results from green channel in our experiments.

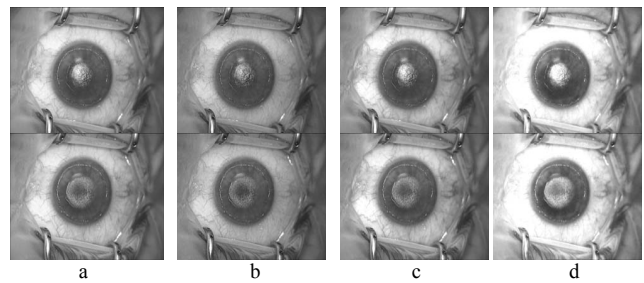


Figure 2: a) Grey level image, b) Red channel, c) Green channel, d) Blue channel.

Human eye makes spherical movement and camera used in capturing dataset images has undesired movement during the surgery. These constraints make difficult to create a geometrical model from obtained images. Therefore, we applied a pre-processing step on the reference image. If the region of interest (ROI) can be identified with approximate iris region boundaries, error rate can be reduced and limited number of interest points can contribute the system performance. Iris has more apparent intensity than other parts. Briefly, cutting this region’s connection from image edges and cleaning small fragments give us approximate iris region. Figure 3 shows the outputs of morphological operations applied on the reference image to find the region of interest. After changing the image to binary, dilation and closing with disc structure element (SE) and then erosion with line SE is applied. After deleting edge connected components, the image is dilated and eroded with a larger disc SE. As a last step, ROI is obtained by taking the difference of dilated and eroded images.

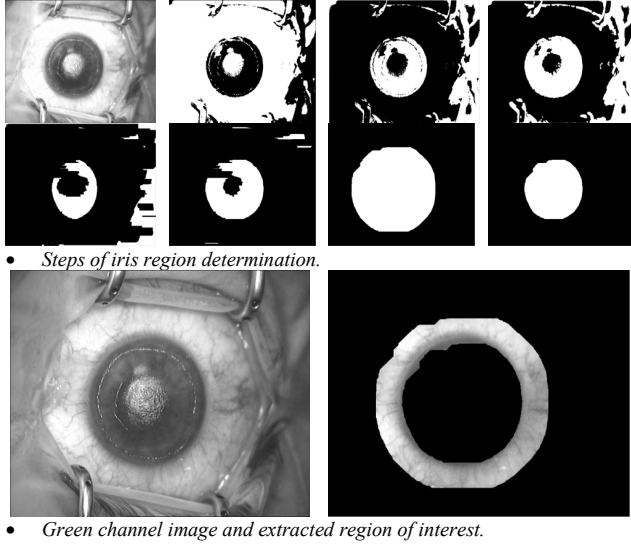


Figure 3: Region of interest extraction from the reference image.

C. Feature Extraction and Matching

After finding the region of interest, distinctive features are extracted from images. We apply SIFT algorithm on the whole image and select interest points in ROI to reduce number of keypoints and eliminate the edge effects. SIFT descriptors are directly used without modification. Extracted keypoints are stored in memory for future matching of subsequent images. Then, SIFT is applied to green channel of subsequent images. When processing subsequent images, we do not need to extract ROI.

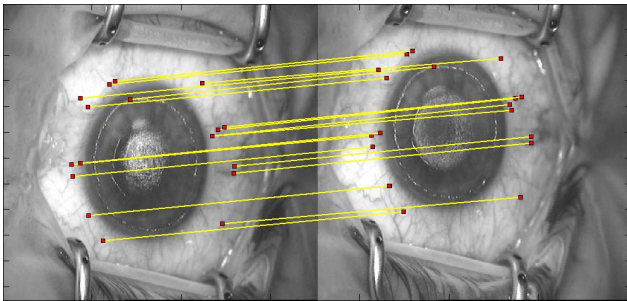


Figure 4: Matched interest points.

Second closest neighbor approach is used for matching feature vectors of the reference and subsequent images. A threshold value is selected in the range of 0.0-1.0. Euclidian distances between a feature of the reference image and all features of the subsequent image are calculated. Two closest matches are selected. If the smallest distance is smaller than the second smallest distance product threshold, the smallest distance feature is a valid match. Otherwise, the feature is discarded. *Figure 4* shows matches between the reference image and a subsequent image.

D. Model Fitting

We define a mask to represent the ablation pattern (*Figure 5(a)*). This mask has sharp edges for faster control fitting performance. As mentioned in Section 3, the object recognition/tracking method in [10] is used for our stabilization approach. To improve the matching performance, Hough transform [11] is applied on feature pairs. Outliers are discarded to reduce our features to a more stable set. Then, RANSAC (Random Sample Consensus) [12] fitting method is applied on this set and an affine matrix is obtained. The affine matrix, which contains translational and rotational transformations, gives us the perspective changes between two images. The information obtained from this matrix is used for mask (*pattern*) registration on subsequent images (*Figure 5(c-d-e-f)*).

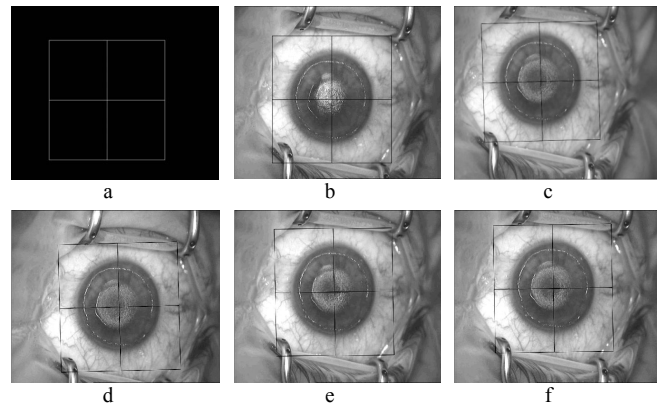


Figure 5: (a) Mask used to represent pattern, (b) Mask on the reference image (c-d-e-f) Mask on subsequent images.

IV. EXPERIMENTAL RESULTS

The input images contain some noise and illumination problems since they were obtained from a non-high speed/non-IR camera. This made our testing more complicated and challenging. To determine the matching performance of our approach, we evaluate the expected and measured position and rotation of the mask (*pattern*) center. The expected pattern position is determined by hand-marking of the observer. Since corneal area deformed during the surgery, we measure the expected values of top, down, left, right coordinates of pattern and then get their mean values to calculate the center position. *Table 1* and *Table 2* list the position and rotation error of center coordinates for a part of our datasets respectively.

In our datasets, an iris has approximately 12-14 mm diameter and is represented by about 300 pixels (45 μ m/pixel). Among the dataset images, the center of pattern moves \sim 2000 μ m (43 pixels) on average. Position error is the Euclidean distance between the expected and measured coordinates in pixel and μ m scales. The average error in our results is \sim 65-70 μ m where the acceptable error

of pattern decentralization should be under 250 μm [14,15]. Rotation errors given in Table 2 are the angular difference between the measured and expected centers (negative values represent counterclockwise angles).

Table 1: Expected (Exp.) and measured (Msr.) center coordinates and the error rate.

Exp. Center (x,y)	Msr. Center (x,y)	Error (pixel)	Error (μm)
330.01,266.50	327.01,267.50	3.16	142.23
326.52,257.00	323.84,257.50	2.74	123.08
288.54,245.98	286.51,245.48	2.09	94.10
356.48,316.01	356.51,315.98	0.04	1.76
342.01,251.00	341.51,250.48	0.72	32.50
345.01,292.50	345.51,293.00	0.71	31.82
339.49,278.49	338.50,279.50	1.41	63.62
355.01,275.00	354.50,276.00	1.12	50.47

Table 2: Expected (Exp.) pattern rotation, measured (Msr.) rotation and error.

Exp. Rotation (degree)	Msr. Rotation (degree)	Error (degree)
-0.46	-0.67	-0.20
-0.46	-0.88	-0.41
-1.24	-1.55	-0.30
-1.05	-1.63	-0.58
-1.48	-1.30	0.18
-0.46	-0.47	0.01
-0.56	-0.38	0.18
-0.56	-0.47	0.10

Average speed performance for each step of our method is listed in Table 3. If Hough transform is not used and GPU implementation of SIFT [13] is used, operating time barely falls under one second. In this paper we did not focus on speed performance but it can be improved by applying different feature extraction methods or input size reduction techniques.

Table 3: Average speed performances for method steps.

Feature Extraction (SIFT)	~1.650 sec
Feature Extraction (SiftGPU)[13]	~0.380 sec
Feature Matching	~0.005 sec
Hough Transform	~1.100 sec
Model Fitting	~0.450 sec

V. CONCLUSION

In this paper, we presented a pattern stabilization method which can be used in laser eye surgery. Our method is based on extracting features from scleral blood vessels and applying the image processing techniques to track the pattern on patient's eye. Experimental results show that the alignment errors can be reduced to an acceptable level by using our method. For eye registration, scleral blood vessels provide us very consistent features especially considering

the deformation of iris region during the eye surgery and shifting of pupil. Our approach can be used like an eye registration technique before the operation but also can be used at regular intervals during the operation to increase the accuracy of eye tracking.

REFERENCES

- [1] R. A. Applegate, G. Hilmantel, H. C. Howland, E. Y. Tu, T. Starck, E. J. Zayac, "Corneal first surface optical aberrations and visual performance.", *J. Refractive Surgery*, 16, p. 507-514, 2000.
- [2] R. R. Krueger, R. A. Applegate, S. M. MacRae, "Wavefront customized visual correction: the quest for super vision II", p. 201-202, 2004.
- [3] F. Li, S. Munn, J. Pelz, "A model-based approach to video-based eye tracking.", *Journal of Modern Optics*, Volume 55, n 4-5, p. 503-531, 2008.
- [4] D. T. Azar, D. D. Koch, "LASIK Fundamentals, Surgical Techniques, and Complications", 2002.
- [5] E. Donnenfeld, "The pupil is a moving target: centration, repeatability, and registration.", *J. Refractive Surgery*, 20 ,p. 593-596, 2004.
- [6] D. A. Chernyak, "Iris-based cyclotorsional image alignment method for wavefront registration", *IEEE Transactions on Biomedical Engineering*, Volume: 52, Issue: 12, p. 2032-2040, 2005.
- [7] H. Kim, J. Choun-Ki, "Ocular cyclotorsion according to body position and flap creation before laser in situ keratomileusis", *Journal of Cataract & Refractive Surgery*, Volume 34, Issue 4, April 2008, p 557-561.
- [8] A. Harden, B. Dulley, "Cyclotorsion: A New Method of Measurement", *Proc. Roy. Soc. Med.* Volume 67, 1974.
- [9] D. G. Lowe, "Distinctive image features from scale-invariant keypoints", *International Journal of Computer Vision*, 60, 2, p. 91-110, 2004.
- [10] D. G. Lowe, "Object recognition from local scale-invariant features, *International Conference on Computer Vision*", Corfu, Greece, pp. 1150-1157, 1999.
- [11] D. H. Ballard, "Generalizing the Hough Transform to Detect Arbitrary Shapes, *Pattern Recognition*", Vol.13, No.2, p.111-122, 1981.
- [12] M. A. Fischler, R. C. Bolles, "Random Sample Consensus: A Paradigm for Model Fitting with Applications to Image Analysis and Automated Cartography", *Comm. Of the ACM* 24: p. 381-395, 1981.
- [13] W. Changchang, "SiftGPU: A GPU Implementation of Scale Invariant Feature Transform", www.cs.unc.edu/~ccwu/siftgpu/.
- [14] S. Amano, S. Tanaka, K. Shimizu, "Topographical evaluation of centration of excimer laser myopic photorefractive keratectomy", *J. Cataract Refract Surg.* 20(6):616-9. PubMed PMID: 7837071, 1994.
- [15] H.B. Çakmak, N. Çağıl, H. Simavlı, D. Dal, S. Bayhan, Ş. Şimşek, "How Does Ablation Decentration Effect Postoperative High Order Aberrations After Miyopic PRK?", *T. Oft. Gaz.*,vol. 39, 189-196, 2009.